The ability of uniform viscous flow under rollers and spreaders

By J. R. A. PEARSON
Imperial Chemical Industries Limited, Akers Research Laboratories,
The Frythe, Welwyn, Herts.†

(Received 24 July 1959)

When a thin film of viscous fluid is produced by passing it through a small gap between a roller or spreader and a flat plate, it often presents a waved, or ribbed, surface. An analysis is given here in terms of lubrication theory to show why in many cases flow leading to a uniform film is unstable. Account is taken of surface tension which proves to be a stabilizing factor. The most unstable values of the wave-number, n (characterizing the disturbance), are calculated as functions of the dimensionless variable $T/\mu U_0$, and of the geometry of the system; T is the surface tension, μ the viscosity and U_0 a representative velocity of the fluid. For the particular case of a spreader in the form of a wide-angled wedge, these predictions are compared with experimental observations. Agreement is obtained for values of $T/\mu U_0$ between about 10 and 0·1, but for smaller values of $T/\mu U_0$ it is clear that other considerations, involving only viscous and pressure forces, determine the nature of the secondary flow.

1. Introduction

Attempts to produce uniform thin layers of very viscous fluid by rolling or spreading often lead to an uneven or ribbed surface. Reference to this phenomenon has been made in a variety of contexts; reports have come from the tinplate industry (Evans & Hoare 1941), the printing ink (Sjodahl 1951), the photographic, [illegible] paint industries (private communications), while the matter has been discussed in the correspondence columns of the *New Scientist* (Letters, Nos. [illegible]).

The [illegible]ader will perhaps be most familar with the case of 'brush marks', which occur when thick paint is applied to a flat surface by means of a bristle brush. The resultant film, especially when just formed, usually presents a waved or ribbed surface where the lines of crests and troughs run roughly parallel to the direction of motion of the brush (see figure 1 *a*, plate 1). A similar ribbing phenomenon can be observed when films of highly viscous fluid are formed by passing the fluid through a small gap under large solid rollers; if the roller is moved perpendicular to its axis over a flat plate, without rotation, the operation is termed *spreading*; if the roller is rolled over the surface, the operation is termed *rolling* (see figure 1 *b*, *c*). A diagrammatic indication of the method used for spreading and of the nature of the resulting film is given in figure 2. A more exact

† Now at The Metal Box Co. Ltd., Technical Engineering Division, Borehamwood, Herts.

indication of the shape of the meniscus in the region where the free surface forms is given also diagrammatically in figure 3 (see also figure 1*e*).

Early quantitative experiments were carried out by A. J. G. Shaw (private communication) of the Research Department, Paints Division, Imperial Chemical Industries Limited, on a series on viscous liquids. Using circular cylindical rollers,

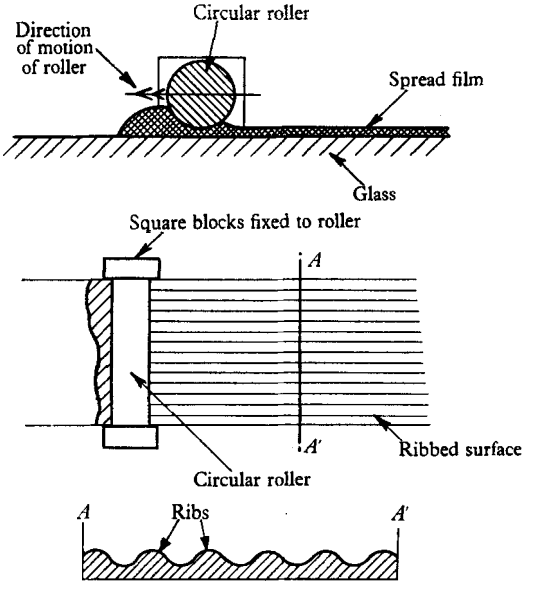

FIGURE 2. The ribbing of a spread film.

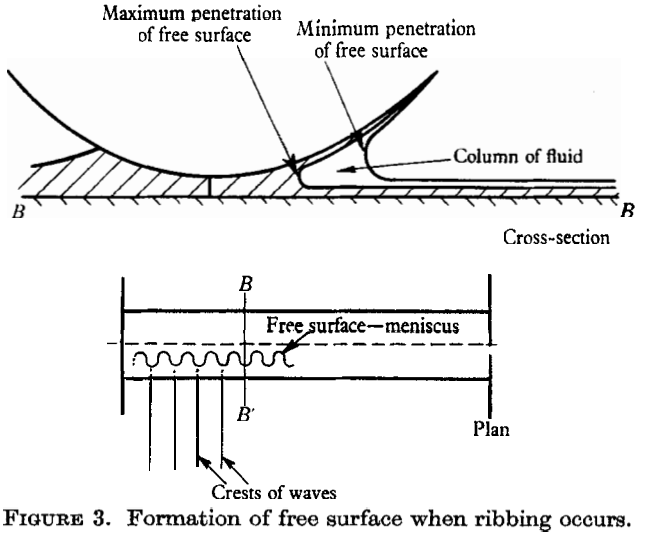

FIGURE 3. Formation of free surface when ribbing occurs.

of radii $\frac{3}{8}$, $\frac{3}{4}$ and $1\frac{1}{2}$ in., he produced layers of thicknesses varying from 0·0005 to 0·016 in. both by rolling and spreading. The viscosities of the liquids varied from about 5 to 300 P and the velocities of spreading and rolling were of the order of 1–20 in./sec. In all cases of spreading and for relatively slow rolling he observed

that the emergent film was covered by regularly spaced lines of crests and troughs running parallel to the direction of motion of the roller. He was able to measure a characteristic wavelength for each set of conditions. In the case of rapid rolling the pattern became more confused with lines lying at varying small angles across the direction of motion. He found that for any given spreader (or roller) and given minimum gap width—in other words for any given geometrical configuration—these patterns were remarkably reproducible. The line spacing (wavelength) remained roughly constant whatever the translational velocity, U_0, of the spreader (or roller) provided that it was sufficiently large to produce well-defined ribbing; as a result, he did not measure this velocity specifically. The patterns seemed to depend very little on the fluid used, provided that it was sufficiently viscous; there was, nevertheless, a small systematic variation with viscosity. Altering the minimum gap width or the radius of the roller did, however, have a marked effect on the wavelength and this dependence was measured for the range of values mentioned earlier. An example of the relation observed between line spacing—expressed as the number of crests per inch, n_0, and minimum gap thickness, h_0, for a roller of $\frac{3}{4}$ in. radius is shown in figure 4. The curves for three liquids both spread and rolled are given.

Other experiments were also carried out by E. Pitts and J. Greiller (private communication) of the Research Department, Kodak Limited on a pair of rotating rollers separated by a small gap and partially immersed in a bath of viscous fluid. In this arrangement the fluid was carried out of the bath between the rollers, and then split into a layer on each roller, thus being returned to the bath as the roller rotated. In this way a steady-state system could be achieved. They found that for sufficiently low rates of rotation a uniform two-dimensional flow was obtained, and that as the rate of rotation of the rollers was increased, a critical value was reached at which the flow became unstable and a ribbed structure similar to that described above was observed. The wavelength of the wave structure obtained was found to decrease—apparently in a discrete series of jumps—as the rate of rotation was further increased. The peripheral roller speeds used by Pitts and Greiller were in general lower than any used by Shaw.

Dimensional considerations suggest that in the experiments described above, the various forces acting can be characterized in the following way:

$$\text{viscous forces} = O(\mu U_0/h_0^2),$$

$$\text{inertia forces} = O(\rho U_0^2/h_0),$$

$$\text{gravity forces} = O(\rho g),$$

$$\text{surface tension forces} = O(T/h_0^2),$$

where ρ is the density of the fluid, g is the gravitational acceleration, T is the surface tension of the fluid and U_0, h_0 and μ are as defined earlier. If h_0 is sufficiently small then viscous and surface tension forces dominate, and if further μU_0 is large compared with T then viscous forces alone dominate. The characteristics common to all the industrial observations on ribbing mentioned earlier were that the gaps, h_0, were very small and that the fluids were very viscous. The experiments of Shaw were such that viscous forces dominated everywhere, while those of Pitts

and Greiller were such that viscous and surface tension forces were of comparable effect.

This suggests that a theoretical treatment should be based on the equations of slow viscous motion, neglecting inertia and gravity forces, and that the effects of surface tension should be included in the boundary conditions.

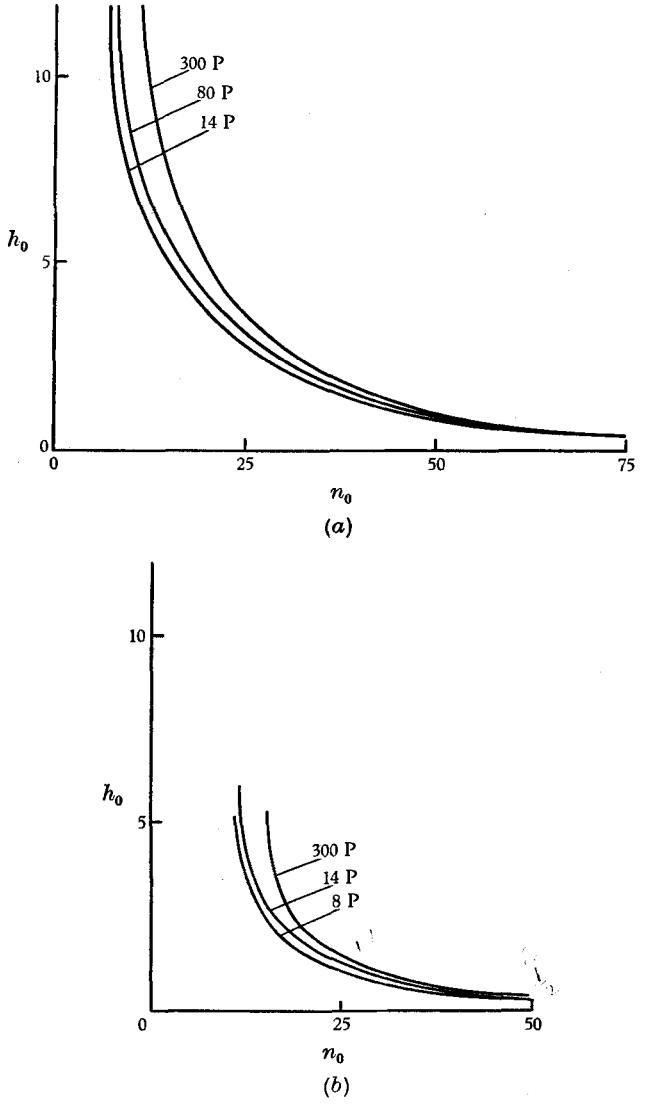

FIGURE 4. n_0, the number of crests per inch, as a function of h_0, the minimum gap thickness in $\frac{1}{1000}$ in., using a $\frac{3}{4}$ in. radius roller. (*a*) Spreading. (*b*) Rolling.

We present here an analysis based on the hydrodynamic theory of lubrication, which is an approximate theory of slow viscous motion applicable to the flows we are considering. The effect of surface tension on the free-surface boundary condition has to be introduced in a simplified, semi-empirical form, because of the limitations inherent in the lubrication equations.

We look first for a possible two-dimensional steady-state solution, that is a solution corresponding to a uniform plane emergent sheet. We find that the equations and boundary conditions we have chosen lead to a degree of arbitrariness in this solution.† Assuming, however, that one of this class of solutions will be relevant, we then study the stability of such flows to three-dimensional disturbances of the type observed in practice. We find that the stability of the system is a function both of its geometry and of the single dimensionless parameter $T/\mu U_0$; surface-tension forces exert a stabilizing influence on an otherwise wholly unstable flow. This general analysis is given in §2. We obtain expressions for the amplification factor, s, as a function of wave-number, n, of the postulated disturbance.

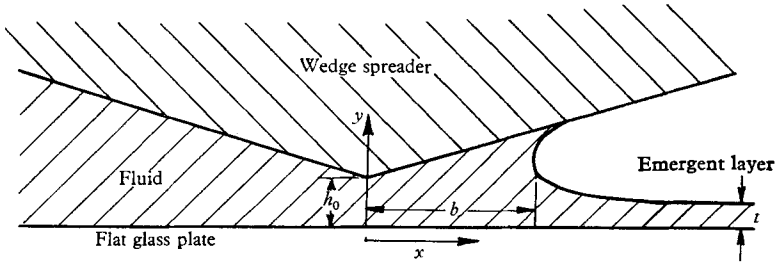

FIGURE 5. The wide-angled wedge spreader.

In order to obtain solutions in terms of tabulated functions, a particularly simple geometrical arrangement is treated in detail in §3. This consists of a wide-angled wedge spreader, illustrated diagrammatically in figure 5. For any specific value of $T/\mu U_0$, and a suitably chosen value of b_0 (the point of furthest penetration of the meniscus), the value of n that maximizes s can be calculated. We assume that this is the value of n that would be observed in practice.

Experiments have been performed in these laboratories using a wedge-shaped spreader to compare the results obtained experimentally for n with those predicted on the basis of the theory outlined above. These also are described in §3. The agreement is good for values of $T/\mu U_0$ between 0·1 and 10.

It is concluded in §4 that the elementary analysis we have used involving surface tension is adequate to describe the ribbing that occurs when $T/\mu U_0$ is appreciable, but that other viscous effects, not included in the lubrication theory, would have to be considered in order to describe the secondary flow that takes place in the limiting case of $T/\mu U_0 \to 0$.

2. General analysis

The conditions encountered in flow under a roller or spreader, where the fluid is supposed incompressible, are precisely those to which the theory of lubrication applies (see, for example, Lamb 1932, Ch. XI). In this approximation, designed to deal with the motion of viscous fluid contained in the narrow regions between nearly parallel moving surfaces, inertia and acceleration terms are neglected, while pressure variations in directions at right angles to the moving surfaces are

† Pitts (1959) has developed an approximate analysis for predicting the point to which the meniscus will penetrate as a function of the dimensionless group $T/\mu U_0$.

assumed to be unimportant. This means that a two-dimensional flow (of the type shown in figure 6) can be represented by a one-dimensional model, while the more complicated three-dimensional flow that results from the ribbing considered in § 1 can be represented by a two-dimensional model. This approximation can be regarded as adequate except in the regions where a meniscus forms, e.g. the line $x = b$ in figure 6. This is because the parabolic type of flow which is relevant for regions far from the meniscus, where the gap is completely filled with fluid, changes sharply, in the region close to the meniscus, into uniform flow (with a free surface) along the two separating surfaces. The latter flow also satisfies the lubrication equations, but in a trivial sense only. The length (in the x-direction)

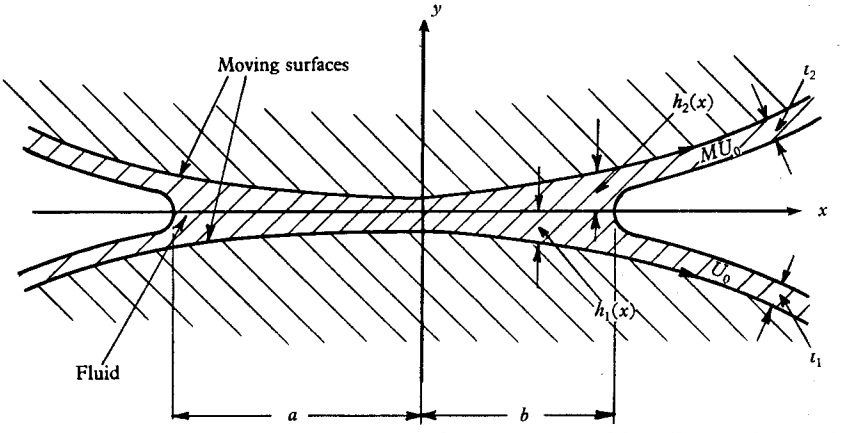

FIGURE 6. Section of flow in the narrow gap between two arbitrarily moving surfaces.

of the region directly affected by the meniscus will be of the order of the gap width at that point and is therefore small compared with other lengths involved, such as b or the line spacing on the emergent sheet.†

In this analysis we shall attempt to represent the whole effect of the meniscus formed at $x = b$ by boundary conditions to be imposed on the lubrication equations at what we shall term a free boundary; this free boundary will for simplicity also be taken to be at $x = b$. Our mathematical model (see figure 7) will therefore consist of two regions (neglecting for the moment the presence of a meniscus at $x = -a$): (i) $x < b$, where the gap is full of liquid and where the lubrication equations apply, and (ii) $x > b$, consisting of two fluid layers of constant width moving with uniform velocity separated by an air gap.

Although changing discontinuously the flows in these two regions must be matched. This is the crux of the problem: we must choose two suitable boundary conditions for the lubrication equations. There must be a mass-flux boundary condition which equates the amount of fluid reaching the free boundary from region (i) to the amount of fluid leaving the free boundary into region (ii). There must also be a pressure boundary condition, the pressure in region (i) at the free boundary being balanced by the sum of the (constant) pressure in region (ii) and the effect of surface tension forces acting on the free boundary. The particular conditions adopted in the following analysis will be discussed when they are chosen.

† This remark is based on empirical observations.

2.1. *Steady two-dimensional flow*

To preserve the utmost generality in this treatment we consider the arrangement shown diagrammatically in figure 6. The two moving cylindrical surfaces are given by $y = h_1(x)$ and $y = h_2(x)$, *where* $h_1'(x)$ *and* $h_2'(x)$ *are everywhere small compared with unity.* (The primes denote differentiation with respect to x.) The tangential velocities of the two surfaces are given by U_0 and MU_0 as indicated

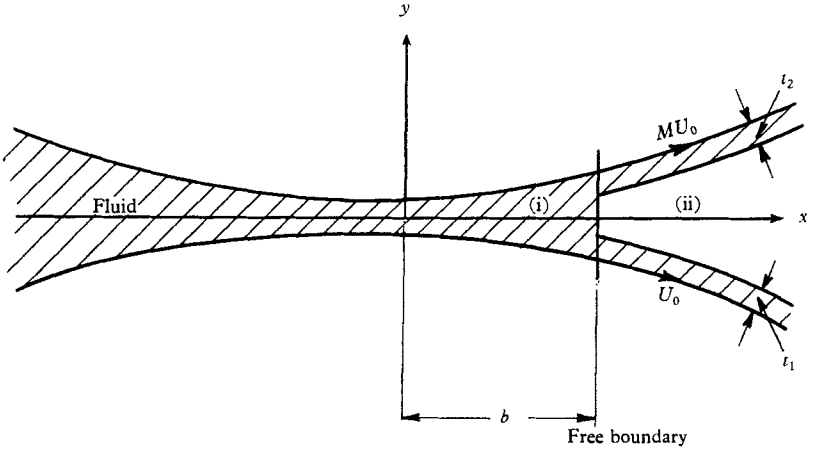

FIGURE 7. Mathematical model of flow shown in figure 6.

($0 \leqslant M \leqslant 1$). Using the usual assumptions of lubrication theory, we find that in the steady state the velocity in the x-direction must be of the form

$$u(x,y) = U_0\left\{\frac{h_2(x)-Mh_1(x)}{h_2(x)-h_1(x)} - \frac{(1-M)y}{h_2(x)-h_1(x)} + \frac{[h_2(x)-y][y-h_1(x)]}{[h_2(x)-h_1(x)]^2}E(x)\right\}, \quad (1)$$

where $E(x)$ remains to be determined. The total mass flux, $U(x)$, between the two surfaces for unit width in the z-direction (perpendicular to the x- and y-axes) at a section x is given by

$$U(x) = \int_{h_1(x)}^{h_2(x)} u\,dy = \tfrac{1}{2}U_0[h_2(x)-h_1(x)][1+M+\tfrac{1}{3}\{E(x)\}]. \quad (2)$$

By continuity this must be constant, and if t_1 is the ultimate film thickness as $x \to \infty$ on surface 1 and t_2 the thickness on surface 2, then

$$U(x) = U_0[t_1 + Mt_2]. \quad (3)$$

This is our first boundary condition. (t_1 and t_2 are the film thicknesses used for region (ii) in our model.)

The equation of motion is given by

$$\frac{dp}{dx} = \mu\frac{\partial^2 u}{\partial y^2} = -\frac{2U_0\mu}{[h_2(x)-h_1(x)]^2}E(x), \quad (4)$$

where p is the pressure and μ the dynamic viscosity. If we assume that the pressure in region (i) at the free boundaries is known, then equation (4) may be integrated using (2) and (3) to give

$$\frac{p(b)-p(-a)}{6\mu U_0} = \int_{-a}^{b}\left[\frac{(1+M)}{\{h_2(x)-h_1(x)\}^2} - \frac{2(t_1+Mt_2)}{\{h_2(x)-h_1(x)\}^3}\right]dx. \quad (5)$$

Unless further information is provided a large degree of indeterminacy remains, for a, b, t_1, t_2, are all as yet arbitrary and are related by only one equation.

One reasonable simplification is to suppose that $a \to \infty$ and that $p(-a) \to 0$. The pressure outside the liquid is taken to be zero. This corresponds to the case where the surfaces are emerging from a large reservoir of fluid, and is in fact reasonably representative of all the cases that have been examined above.

But the indeterminacy still remaining in the specification of the section at which the free boundary—or meniscus—forms cannot be so simply resolved. The obvious refinement to attempt would be to replace the lubrication equations (1)–(4) by the Stokes slow-motion equations, and seek solutions of these using exact free surface boundary conditions on both velocity and stress. Using a stream function, this leads to the biharmonic equation. Unfortunately, the equation for the surface remains an unknown variable, and it is by no means certain that the solution of this more complicated equation would remove the indeterminacy.

Pitts (1959) has described an approximate method for resolving this indeterminacy that he has applied with some success to the symmetric case of two circular rollers, where $h_1(x) = -h_2(x)$ and $M = 1$. In this he makes use of the experimentally observed fact that the meniscus is parabolic near its intersection with the axis of symmetry; this equivalent parabola he characterizes by r, the length of its latus rectum. He then looks for that value of b (see figure 6) which for suitable r makes the lubrication solution (1) (written in terms of a stream function) satisfy the exact stress boundary conditions on the parabolic surface in the region close to the axis of symmetry. The predicted values of b (for values of $T/\mu U_0$ sufficiently high for the two-dimensional flow to be stable) were compared with experimental observations and fairly encouraging results obtained. Unfortunately, it is not clear how such a method could be applied to the asymmetric case of spreading, and this will not be attempted in §3.

Hopkins (1957) has suggested that the meniscus will form at the first stagnation point (in the case of a sheet moving between two rollers); this seems to be confirmed for the case $T/\mu U_0 \to 0$ both by experimental results and by the approximate theory of Pitts.

Experimentally, the value of b is found to decrease as U_0 is increased (for fixed T and μ) and tends to an asymptotic value, b_∞. This general result is to be expected even on the basis of our approximate treatment, because the lubrication solution yields a region of reverse flow for all b greater than some value b_s, b_s being defined by the geometry alone; we would therefore expect the meniscus to be drawn towards the point b_s, the more so as μU_0 increases with respect to T, and indeed it has been roughly verified that $b_s \doteqdot b_\infty$.

One further remark can be made about the variables in (5) for the particular arrangements that have been studied. For rolling, $M = 1$ and by symmetry we could put $t_1 = t_2$, while for spreading, $M = 0$ and $t_2 = 0$. Thus if we *fix* b, and assume that $p(b)$ is known, then t_1 is given by (5) in terms of known quantities, and $E(x)$ in (2) can be calculated. In this way, specification of b (assuming $a \to \infty$) leads to a complete solution for the velocity $u(x, y)$ in terms of lubrication theory. Little has been said about $p(b)$ so far: the simplest assumption is to put it equal to zero. However, allowance can be made for surface tension effects as will

be seen in later sections, and indeed the inclusion of surface tension effects will be critical to the stability analysis that we shall carry out in the following subsection.

2.2. *The growth of small lateral disturbances*

We now superpose on the given basic two-dimensional steady flow infinitesimal lateral disturbances that are chosen to correspond to those described in §1. Since the equations describing the motion are linear there will be no interaction between the two motions in the main body of fluid. Hence it is the particular choice of boundary conditions that will be of critical importance.

We therefore now consider a non-steady velocity field given by

$$u(x,y,z,t) = U_0\left\{\frac{h_2(x)-Mh_1(x)}{h_2(x)-h_1(x)} - \frac{(1-M)\,y}{h_2(x)-h_1(x)} + \frac{[h_2(x)-y][y-h_1(x)]}{[h_2(x)-h_1(x)]^2}K(x,z,t)\right\}, \tag{6}$$

$$w(x,y,z,t) = U_0\frac{[h_2(x)-y][y-h_1(x)]}{[h_2(x)-h_1(x)]^2}J(x,z,t), \tag{7}$$

where u and w are velocities in the x- and z-directions, respectively. There will be associated mass fluxes

$$U(x,z,t) = \int_{h_1(x)}^{h_2(x)} u\,dy = \tfrac{1}{2}U_0[h_2(x)-h_1(x)][1+M+\tfrac{1}{3}\{K(x,z,t)\}] \tag{8}$$

and

$$W(x,z,t) = \int_{h_1(x)}^{h_2(x)} w\,dy = \tfrac{1}{6}U_0[h_2(x)-h_1(x)]J(x,z,t). \tag{9}$$

Continuity imposes the condition

$$\frac{\partial U}{\partial x}+\frac{\partial W}{\partial z} = 0, \tag{10}$$

whence

$$\frac{\partial}{\partial x}\{(h_2-h_1)(3+3M+K)\}+(h_2-h_1)\frac{\partial J}{\partial z} = 0, \tag{11}$$

while the equations of motion are given by

$$\frac{\partial p}{\partial x} = \mu\frac{\partial^2 u}{\partial y^2}, \quad \frac{\partial p}{\partial z} = \mu\frac{\partial^2 w}{\partial y^2}. \tag{12}$$

We now characterize the disturbance by supposing the free boundary to form at the points

$$b = b_0 + c\,e^{st}\cos nz, \tag{13}$$

where $c \ll 1$ and n is arbitrary. We suppose in consequence that the mass flows will be given by

$$K(x,z,t) = E(x) - cF(x)\,e^{st}\cos nz, \tag{14}$$

$$J(x,z,t) = cG(x)\,e^{st}\sin nz, \tag{15}$$

where $E(x)$ is defined by (2), (3) and (5). By substituting (14) and (15) into (11) and using (2) and (3), we obtain from the continuity relation

$$\frac{\partial}{\partial x}\{(h_2-h_1)F\} = nG(h_2-h_1); \tag{16}$$

by using the equations (12) and eliminating p we get

$$nF = h^2 \frac{\partial}{\partial x}\left(\frac{G}{h^2}\right). \tag{17}$$

where $h = h_2 - h_1$. Finally, we obtain the following second-order linear differential equation for $G(x)$,

$$G'' - \frac{h'}{h} G' - \left(n^2 + \frac{2h''}{h}\right) G = 0. \tag{18}$$

We must now choose two boundary conditions to be imposed at the free boundary given by (13).

The first boundary condition will be obtained by considering the force balance across the free boundary. We can without loss of generality put $p = 0$ in region (ii). If we consider the two-dimensional case represented in figure 7, then the relevant relation is given by

$$p(b)\, h(b) = -2T, \tag{19}$$

where $p(b)$ refers now to the pressure in region (i). This relation is consistent with the lubrication hypothesis in that inertia terms are neglected, and with the concept of a free boundary, thus avoiding any viscous components of stress.† The three-dimensional case must include surface tension components that act in the xz-plane and by using the simplest possible representation we obtain

$$p(b)\, h(b) = -T\left[2 + (h - t_1 - t_2)\frac{\partial^2 b}{\partial z^2}\right]. \tag{20}$$

If we now linearize in c this pressure boundary condition (20) becomes

$$p(b) = -T\left(\frac{2}{h(b_0)} - c\left[\frac{2h'(b_0)}{h^2(b_0)} + n^2\left(1 - \frac{t_1}{h} - \frac{t_2}{h}\right)\right] e^{st} \cos nz\right). \tag{21}$$

We may further assume that

$$p(-a) = 0, \quad G(-a) = 0, \quad F(-a) = 0. \tag{22}$$

This is in keeping with the observation that the lateral variations in layer thickness of the emerging film have no effect on the flow of the fluid in front of the roller or spreader, and the further observation that the nature of the emerging film is independent of the conditions existing in front of the roller or spreader provided only that a is large enough (i.e. $a \gg b$). If we therefore integrate the first of the equations of motion (12), linearize in c, use relations (6), (14) and (21) and subtract out the steady component satisfying (5), we derive our first boundary condition on the time-dependent component. This is

$$G(b_0) = -n\left[E(b_0) + \frac{T}{2\mu U_0}\left\{2h'(b_0) + n^2\left(1 - \frac{t_1}{h} - \frac{t_2}{h}\right) h^2(b_0)\right\}\right]. \tag{23}$$

It is here that dependence on the parameter $T/\mu U_0$ is introduced.

† This simplication was suggested originally by Sir Geoffrey Taylor (see Saffman & Taylor 1958).

A second boundary condition is obtained by relating the rate at which fluid reaches the free surface to the rate at which it is carried away, and to the rate at which the free surface advances. We write

$$m_1(b) = \frac{t_1^*(b)}{h(b)}, \quad m_2(b) = \frac{t_2^*(b)}{h(b)},$$

where t_1^* and t_2^* are the instantaneous thicknesses of the layers formed on surfaces 1 and 2 along lines $z = \text{const}$. (These must not, for the present, be confused with the values t_1 and t_2 considered in the previous section, since a basic unperturbed flow may be possible for one value of b only.) For any value of z, the amount of fluid instantaneously arriving at b is given by

$$\tfrac{1}{2}U_0 h(b)\,[1 + M + \tfrac{1}{3}\{E(b)\} + \tfrac{1}{3}c\{F(b)\}\,e^{st}\cos nz];$$

the amount instantaneously carried away by the surfaces 1 and 2 is given by

$$U_0[m_1(b) + Mm_2(b)]\,h(b);$$

the rate at which the free surface advances is given by

$$\frac{\partial b}{\partial t} = sc\,e^{st}\cos nz.$$

Mass conservation therefore requires that

$$(1 - m_1 - m_2)\,h\frac{\partial b}{\partial t} = \tfrac{1}{2}U_0 h[1 + M + \tfrac{1}{3}E + \tfrac{1}{3}cF\,e^{st}\cos nz] - U_0(m_1 + Mm_2)\,h.\dagger$$

Linearizing and using the steady-state result given by (2) and (3), we get

$$s = \frac{U_0}{1 - m_1(b_0) - m_2(b_0)}\,[\tfrac{1}{3}\{E'(b_0)\} + \tfrac{1}{6}\{F(b_0)\} - m_1'(b_0) - Mm_2'(b_0)] \tag{24}$$

as the second boundary condition. Here the function E, and hence E', is taken to be defined uniquely by (2), (3) and (13) whatever m_1 and m_2. Unfortunately, our whole analysis so far does not enable us to say anything definite about $m_1'(b_0)$ and $m_2'(b_0)$ though we can suppose $m_1(b_0)$ and $m_2(b_0)$ to be known. However, if we use (24) only to select the most unstable wave-number, i.e. that value of n that maximizes s, then the value of the constant term that remains unknown is not relevant.‡ It is only when we use (24) to provide criteria for absolute stability that we need to evaluate this constant.

If we take m_1 and m_2 to be given as functions of b, by equating t_1^* and t_2^* to t_1 and t_2, for all b, then relation (24) becomes simply

$$s = \frac{U_0 F(b_0)}{6\{1 - m_1(b_0) - m_2(b_0)\}}. \tag{24, i}$$

This is equivalent to supposing that all basic unperturbed flows are initially possible. If, on the other hand, we take $m_1'(b_0) = m_2'(b_0) = 0$, which corresponds

† This relation assumes that velocities in the z-direction are not transmitted across the free boundary. This approximation will be valid provided the wavelength $2\pi/n$ is large compared with h. This has been the case in all our observations.

‡ This supposes that m_1' and m_2' are to first order in c independent of n.

to the supposition that the shape of the free surface in the xy-plane for all b will be everywhere geometrically similar, then (24) becomes

$$s = \frac{U_0}{3\{1-m_1(b_0)-m_2(b_0)\}}\{E'(b_0)+\tfrac{1}{2}[F(b_0)]\}. \tag{24, ii}$$

In the application of the theory made in §3 we shall use both of these criteria.

3. The wedge-shaped spreader

In order to study the consequences of the analysis given in the previous section, a particular case, that of a wide-angled wedge, has been worked out in detail and the results compared with those obtained experimentally. The relations (24, i) and (24, ii) have been calculated for various values of $T/\mu U_0$ and b_0 regarding s as a function of n; μ, U_0 and T can be taken as adjustable parameters; b_0 is not prescribed by our elementary theory, but it has been measured experimentally for various values of $T/\mu U_0$. It must be remembered that the analysis of §2.2 is a perturbation analysis and strictly speaking refers only to the growth of small disturbances on a steady two-dimensional flow. If the initial disturbances are very small and are taken to include components at all wave-numbers, then it is reasonable to assume that those wave-numbers which maximize s for given b_0 and $T/\mu U_0$ will dominate the early stages of the instability. But it is not necessarily true that the ultimate steady secondary flow that is attained will be characterized by the same wave-number, although other examples of instability in hydrodynamics suggest that it may be. Nevertheless, since we are unable to carry out a full analysis of the secondary flow, we are bound to carry the comparison as far as we can—on the supposition that agreement between perturbation theory and observation in a range strictly outside that to which perturbation theory applies is better than no agreement at all. Ideally we should restrict comparison to those values of $T/\mu U_0$ for which the flow is just unstable; unfortunately, this range, for the linear dimensions chosen in our experiments, corresponds to that region where gravity forces become appreciable as an additional stabilizing factor. In view of all these uncertainties, it is perhaps rather surprising that the agreement obtained was so good.

3.1. *Analysis*

A diagram of the wedge used is given in figure 5. The equation for the gap width, $h(x)$, is given by

$$h(x) = h_0 + \alpha|x|. \tag{25}$$

The free boundary is supposed to form at $x = b$. (This corresponds to the case $h_1(x) \equiv 0$, $M = 0$, $t_2 = 0$, in §2.1.) We write $t_1 = t$, $\lambda = t/h_0$, $k = \alpha/h_0$.

From (1) we have

$$u(x,y) = U_0\left\{1-\frac{y}{h}+\frac{(h-y)\,y}{h^2}E(x)\right\}, \tag{26}$$

and from (2) and (3)

$$E(x) = \frac{3[2t-h(x)]}{h(x)}. \tag{27}$$

For steady-state flow, we suppose that $a \to \infty$, $p(a) \to 0$, and that $p(b)$ is given by

$$p(b) = -\frac{2T}{h_0(1+kb)}. \tag{28}$$

This is the assumption that we introduced earlier in §2.2. The pressure condition (5) becomes

$$-\frac{T\alpha}{3U_0\,\mu(1+kb)} = \left[\frac{\lambda}{(1+kb)^2} - \frac{1}{(1+kb)} + 2 - 2\lambda\right], \tag{29}$$

and thus $E(b)$ can be written

$$E(b) = \frac{-6(1+kb)^2 + 12(1+kb) - 3 + \tau}{2(1+kb)^2 - 1}, \tag{30}$$

where

$$\tau = \frac{2T\alpha}{\mu U_0} \tag{31}$$

and will be used henceforth as the relevant dimensionless number characterizing the relative effect of viscous and surface tension forces.

The basic equation for small perturbations, equation (18), becomes

$$G'' - \frac{kx}{|x|\,(1+k\,|x|)}\,G' - n^2 G = 0. \tag{32}$$

For $x > 0$, we write $1 + kx = k\eta$ to give

$$\frac{d^2G}{d\eta^2} - \frac{1}{\eta}\frac{dG}{d\eta} - n^2 G = 0 \quad (\eta > k^{-1}),$$

and for $x < 0$, we write $1 - kx = k\zeta$ to give

$$\frac{d^2G}{d\zeta^2} - \frac{1}{\zeta}\frac{dG}{d\zeta} - n^2 G = 0 \quad (\zeta > k^{-1}).$$

These equations have as general solutions

$$\left.\begin{aligned} G &= A_1\eta I_1(n\eta) + B_1\eta K_1(n\eta), \\ G &= A_2\zeta I_1(n\zeta) + B_2\zeta K_1(n\zeta), \end{aligned}\right\} \tag{33}$$

where I_1 and K_1 are modified Bessel functions. If we apply boundary condition (22), then as $x \to -\infty$ and $\zeta \to \infty$, G must $\to 0$. Hence $A_2 = 0$. Also at $x = 0$, G and G' must be continuous. Hence

$$\left.\begin{aligned} B_2 K_1\left(\frac{n}{k}\right) &= A_1 I_1\left(\frac{n}{k}\right) + B_1 K_1\left(\frac{n}{k}\right), \\ -B_2\left[K_1\left(\frac{n}{k}\right) + \frac{n}{k}K_1'\left(\frac{n}{k}\right)\right] &= A_1\left[I_1\left(\frac{n}{k}\right) + \frac{n}{k}I_1'\left(\frac{n}{k}\right)\right] + B_1\left[K_1\left(\frac{n}{k}\right) + \frac{n}{k}K_1'\left(\frac{n}{k}\right)\right]. \end{aligned}\right\} \tag{34}$$

This yields a unique relation between A_1 and B_1. Remembering that we are supposing the free surface to form at the point $b = b_0 + c\,e^{st}\cos nz$, the pressure condition (23) yields the relation

$$\left(\frac{1}{k} + b_0\right)\left[A_1 I_1\left(\frac{n}{k} + nb_0\right) + B_1 K_1\left(\frac{n}{k} + nb_0\right)\right] = -n\left[E(b_0) + \frac{\tau}{2}\left\{1 + \frac{\alpha}{2}(1 - m(b_0))\left(\frac{n}{k} + nb_0\right)^2\right\}\right], \tag{35}$$

where $E(b_0)$ is defined by (30) and $m(b_0) = \frac{1}{6}[E(b_0) + 3]$. Thus A_1 and B_1 are completely specified in terms of b_0, τ and n, using (34) and (35), giving

$$A_1 = -\frac{n[E(b_0)+\frac{1}{2}\tau\{1+\frac{1}{2}\alpha(1-m(b_0))\,([n/k]+nb_0)^2\}]}{\left(\frac{1}{k}+b_0\right)\left[I_1\left(\frac{n}{k}+nb_0\right)+\frac{1}{2}\left\{I_0\left(\frac{n}{k}\right)\left|K_0\left(\frac{n}{k}\right)-I_1\left(\frac{n}{k}\right)\right|K_1\left(\frac{n}{k}\right)\right\}K_1\left(\frac{n}{k}+nb_0\right)\right]},$$

$$B_1 = -\frac{\frac{n}{2}\left[I_0\left(\frac{n}{k}\right)\left|K_0\left(\frac{n}{k}\right)-I_1\left(\frac{n}{k}\right)\right|K_1\left(\frac{n}{k}\right)\right]\left[E(b_0)+\frac{\tau}{2}\left\{1+\frac{\alpha}{2}(1-m(b_0))\left(\frac{n}{k}+nb_0\right)^2\right\}\right]}{\left(\frac{1}{k}+b_0\right)\left[I_1\left(\frac{n}{k}+nb_0\right)+\frac{1}{2}\left\{I_0\left(\frac{n}{k}\right)\left|K_0\left(\frac{n}{k}\right)-I_1\left(\frac{n}{k}\right)\right|K_1\left(\frac{n}{k}\right)\right\}K_1\left(\frac{n}{k}+nb_0\right)\right]}. \quad (36)$$

The equations (24, i) and (24, ii) become

$$s = \frac{U_0\left[A_1\left\{\left(\frac{n}{k}+nb_0\right)I_0\left(\frac{n}{k}+nb_0\right)-2I_1\left(\frac{n}{k}+nb_0\right)\right\}+B_1\left\{\left(\frac{n}{k}+nb_0\right)K_0\left(\frac{n}{k}+nb_0\right)+2K_1\left(\frac{n}{k}+nb_0\right)\right\}\right]}{6n[1-m(b_0)]} \quad (37, \text{i})$$

and

$$s = \frac{U_0\left[2nE'(b_0)+A_1\left\{\left(\frac{n}{k}+nb_0\right)I_0\left(\frac{n}{k}+nb_0\right)-2I_1\left(\frac{n}{k}+nb_0\right)\right\}+B_1\left\{\left(\frac{n}{k}+nb_0\right)K_0\left(\frac{n}{k}+nb_0\right)+2K_1\left(\frac{n}{k}+nb_0\right)\right\}\right]}{6n[1-m(b_0)]}, \quad (37, \text{ii})$$

where A_1 and B_1 are given by (36).

Because of the arbitrariness in b_0, we are not able to present complete stability diagrams, that is curves for s as a function n and τ, from theoretical considerations alone. Thus we cannot predict in advance that the motion will always be stable for all $\tau >$ some τ_{crit} and unstable for $\tau < \tau_{\text{crit}}$, even though experimental observations suggest that this is true. Our mathematical model must use empirical information if it is to be compared with experimental results.

Some typical examples of the curves obtained from (37, i) and (37, ii) are given by figure 8. Three separate values of τ have been chosen; for each of these, values of b_0 which correspond to those observed experimentally (for particular values of α and h_0) have been used. Figure 9 attempts to show how $n(s_{\max})$ (where $n(s_{\max})$ refers to that value of n that maximizes s) varies with b_0 for fixed τ: it is a fairly typical curve and shows how little $n(s_{\max})$ varies over quite a wide range of b_0 which includes the observed value.

It can be seen that for all values of b_0, the hypothesis (i) leads to a more unstable situation than hypothesis (ii); this conclusion is fairly obvious on physical grounds since the second hypothesis supposes that increasing b_0 increases t much more rapidly than does the first.

The behaviour of s in the limit $n = 0$ is of some interest; the relevant relations that follow from (37, i) and (37, ii) are

$$s = \frac{U_0[2E(b_0)+\tau]}{6[1-m(b_0)]\,[(1/k)+b_0]}, \quad (38, \text{i})$$

and

$$s = \frac{U_0}{6[1-m(b_0)]}\left[E'(b_0)+\frac{2E(b_0)+\tau}{\{(1/k)+b_0\}}\right]. \quad (38, \text{ii})$$

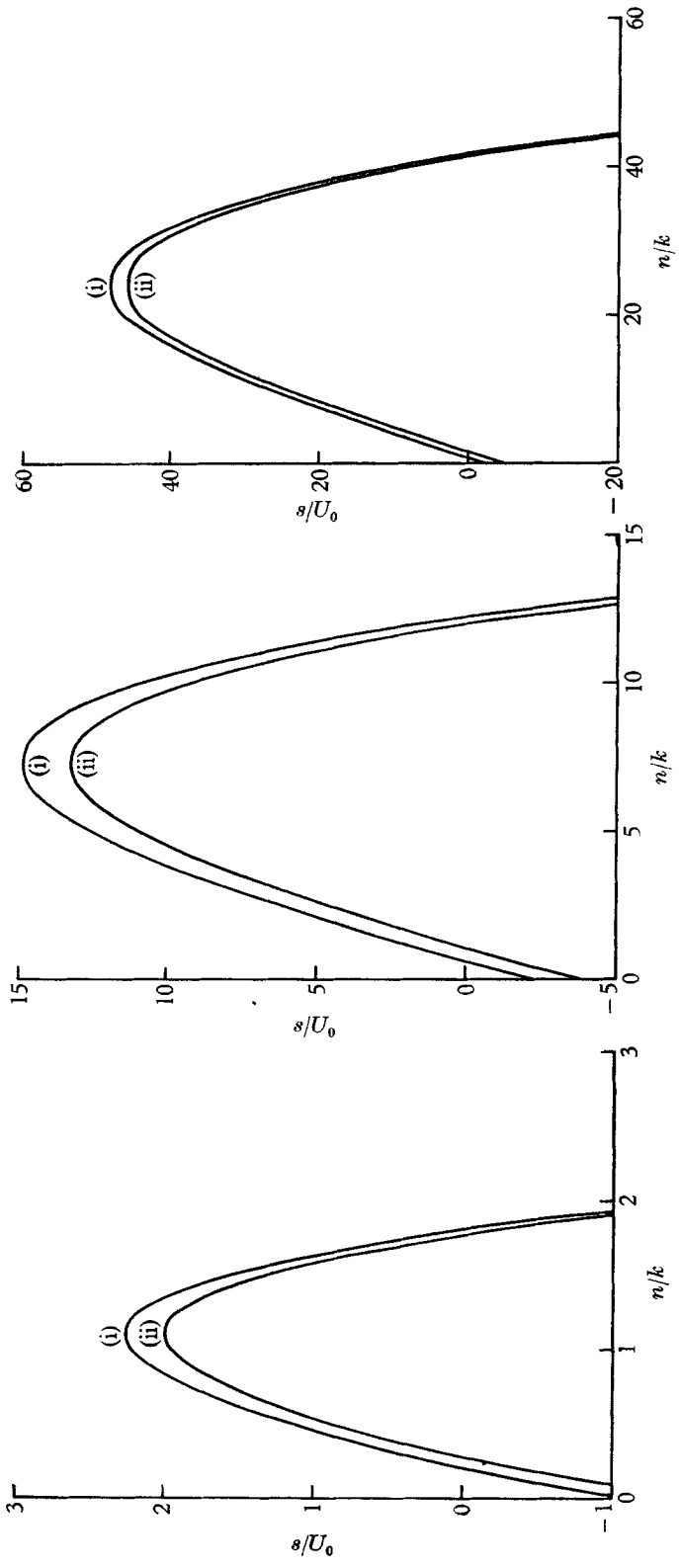

FIGURE 8. Growth rate, s/U_0, as a function of wave-number, n/k, using hypotheses (i) and (ii) for: (*a*) $\tau = 1$, $b_0 = 0{\cdot}48$; (*b*) $\tau = 0{\cdot}1$, $b_0 = 0{\cdot}16$; (*c*) $\tau = 0{\cdot}01$, $b_0 = 0{\cdot}13$.

(38, i), and hence our mathematical model, implies that for all τ, there exists a b_{crit} such that $s > 0$ for all $b_0 \leqslant b_{\text{crit}}$, while (38, ii) implies a range of instability that is contained within that obtained using (38, i). It can be argued that our supposed steady-state two-dimensional flow should never be characterized by a b_0 lying within the range of instability for zero wave-number disturbances, and indeed it was found that the observed values of b_0 always satisfied this condition.

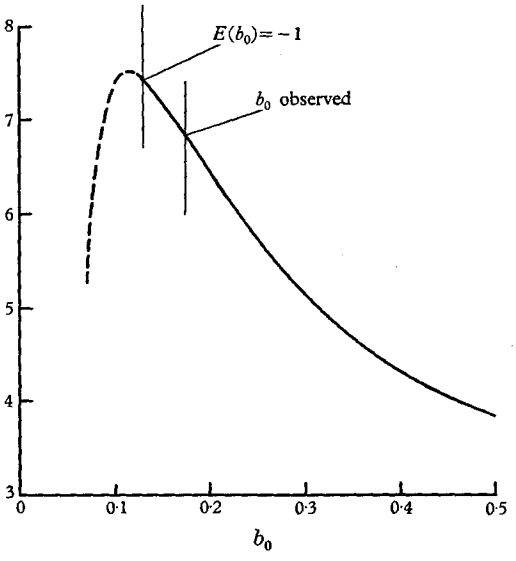

FIGURE 9. $n(s_{\max})/k$ as a function of b_0 for $\tau = 0{\cdot}1$.

3.2. *Experimental results*

For the purposes of experiment a compromise had to be made between
of h_0 and α sufficiently large to allow of accurate machining and sufficientl
to ensure the validity of the lubrication equations and of our free bo
hypothesis. With this in mind, the values $h_0 = 0{\cdot}004$ in. and $\alpha = 1/20$ were
Furthermore, the spreader could only be of limited size. The wedge was
nated at $x = 1$ in. and $x = -1$ in. (using the notation of figure 5) by vertical
and was some 6 in. wide in the z-direction. It was drawn, at measured con
speed, across a plate-glass sheet by a geared-down electric motor, a side fl
ensuring that its motion was perpendicular to planes $x = \text{const}$. Instantane
flash photographs were taken from underneath the plate to measure b_0
example of which is given in figure 1 *e*; photographs taken from above by tr
mitted light were used to measure the line spacing, and an example of the
given in figure 1 *d*.

Experience with circular rollers of different lengths suggested that the li
tion on size in the z-direction would not have any appreciable effect, while
truncation of the wedge at $x = -1$ was only expected to have noticeable effec
the lower speeds. This can be seen by solving equation (32) using a non-infinite
value for a in (22); the effect is not large provided n is not small. The patterns of
lines obtained, although not absolutely regular on any photograph, were repro-

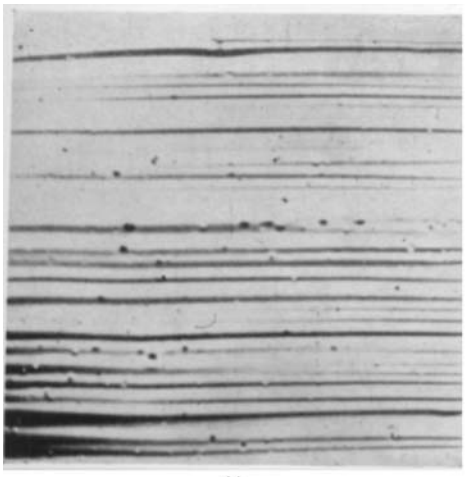

(*a*)

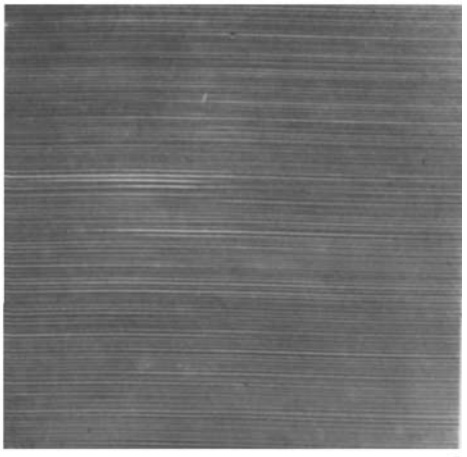

(*b*)

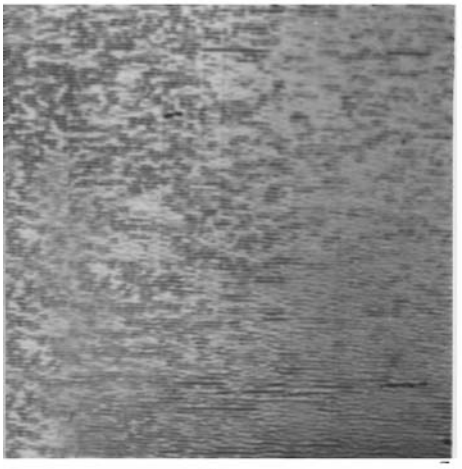

(*c*)

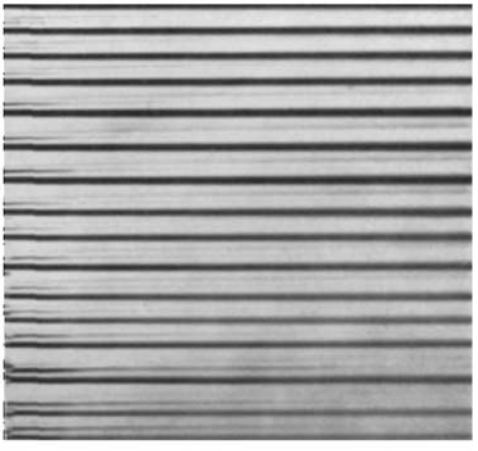

(*d*)

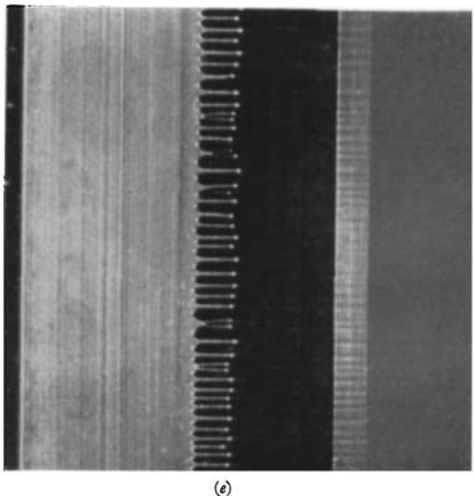

(*e*)

FIGURE 1 (plate 1). (*a*) Brush marks—bristle brush. (*b*) Spread film—circular roller. (*c*) Rolled film—circular roller. (*d*) Spread film—wedge spreader. (*e*) Under view of wedge spreader during experiment.

ducible and yielded satisfactory estimates for n in each case. Three fluids were used; they are tabulated with their relevant physical properties below.

Liquid	Viscosity (poise at 23 °C)	Surface tension (c.g.s. units)
I.C.I. silicone oil F 110/1000	14·5	21
Analar glycerol	11·6	63
B.D.H. glycerol diluted with water	2·7	57

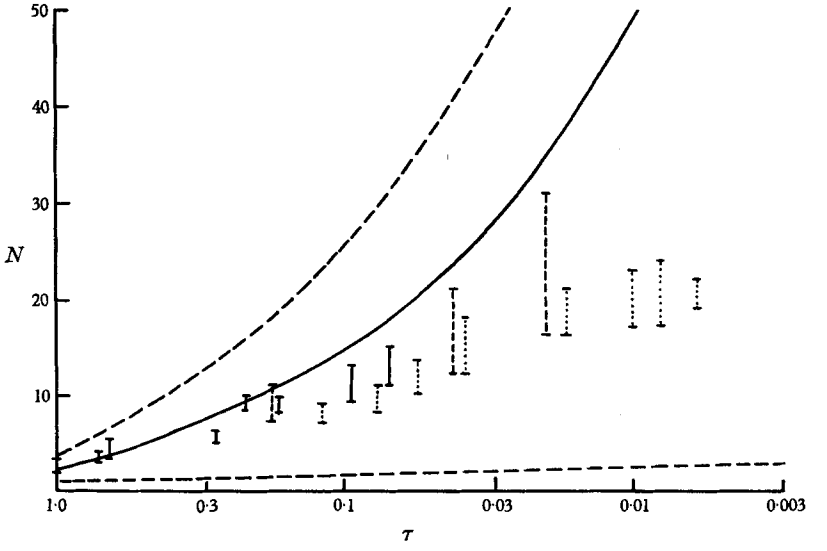

FIGURE 10. N, the number of crests per inch, as a function of τ—comparison between calculated range of instability and observed values. ----, calculated neutral stability curve; ——, calculated $n(s_{\max})$; I, glycerol; 3P; I, glycerol 12P; I, silicone oil 15P.

The combined results are presented in figure 10 were $n_{(\text{observed})}$ is plotted as a function of τ. The values of $b_{0(\text{observed})}$ are plotted as a function of τ in figure 11.

Owing to the large variation of viscosity with temperature and with water content of glycerol, and to the difficulty of preventing surface contamination and hence a reduction in effective surface tension, the calculated values for τ are subject to a rather large margin of error, possibly even 20 % in some cases. This does not mean that quantities were not measured accurately or that reasonable precautions were not taken where necessary, but it allows for the occasions when conditions happened to change between measurements of relevant physical quantities. Indeed, it is worth pointing out that extreme care was taken to polish the glass plate and to clean the metal surfaces on the wedge before each experiment and that fresh glycerol was used every time.

3.3. *Comparison of theory and experiment*

Because the analysis of §2.1 does not prescribe a value of b_0 for any particular choice of τ, we have used the observed values of b_0 as a starting point for the

perturbation calculations. Figure 11 shows the results obtained and compares them with the values that would have been predicted supposing the free surface to form at the point where reverse flow is just about to take place, namely where $E(b_0) = -1$. It is seen that as τ decreases the two curves tend to coincide. This is in agreement with the observations of Pitts and Greiller on two revolving rollers and is the analogue of Hopkins's postulate. It can equally be verified that $b_0 > b_\infty$ (see §3.1) in all cases.

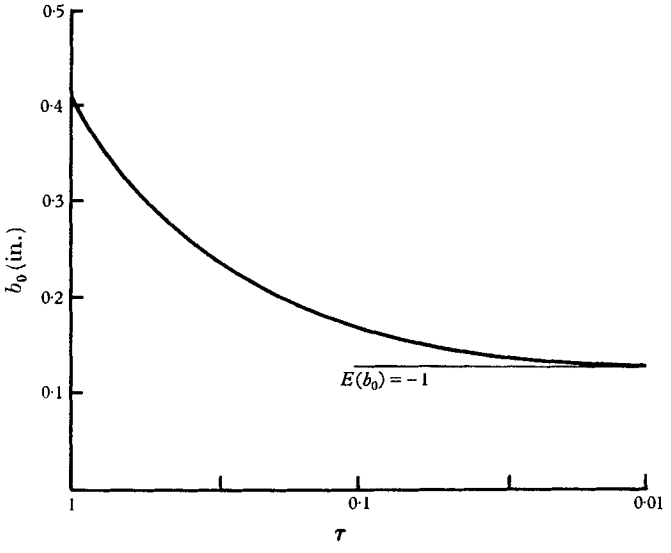

FIGURE 11. b_0 *vs* τ—observed values.

The results of the calculations based on (38, i) and (38, ii) are shown in figure 8, for three particular values of τ ($\tau = 1$, 0·1 and 0·01) and appropriate values of b_0. These give an indication of the large range of wave-number that is likely to be unstable. A more comprehensive indication of the predictions is given in figure 10 where $n(s_{\max})$ and the entire range of unstable n are plotted as functions of τ. The width of the band is a function of the form assumed for $m'(b)$ in (37) and in this figure the means of values obtained by hypotheses (i) and (ii) have been plotted. Also shown on this figure are the observed values of n, mentioned in the previous section. The agreement over a wide range of τ is encouraging. It will be noticed that neither the calculations nor the experimental observations are given beyond the point $\tau = 1$. From the experimental point of view it was clear that a critical value did exist for τ ($\tau \sim 3$) above which the two-dimensional flow was stable; however, the amplitude of the ribbing for values of τ just below this critical value was so small that measurement of wave-number became extremely difficult; this also made it difficult to determine the critical point exactly. Also, in our preliminary discussion of various forces that might be relevant, we showed by dimensional considerations that gravity forces would be small compared with viscous and/or surface tension forces, provided h_0 were small enough. This result, like many dimensional arguments, is only partially true. If U_0 becomes sufficiently small, then the relevant length scale is not h_0 but $h(b_0)$, and the ratio between

viscous and gravity forces is given by $\mu U_0/h^2\rho g$ and between surface tension and gravity forces by $T/h^2\rho g$. In our particular observations, when

$$\tau = 1, \quad \mu U_0/h^2\rho g = 1, \quad T/h^2\rho g = 10,$$

and gravity forces are thus of the same order of magnitude as viscous forces. To emphasize this fact we have deliberately truncated figure 10 at $\tau = 1$.

As τ tends to zero, the observed value of n is seen to tend to a constant value. Because of the extremely high value for viscosity, or the extremely high value for velocity involved at low values of τ, reproducible steady flows were difficult to obtain with the given length of glass plate. In fact, b_0 was observed to vary between experiments; interestingly enough the values recorded for n varied simultaneously in the manner suggested by figure 11.

4. Discussion

The comparison made in § 3.3 for the special case of the wedge-shaped spreader suggests strongly that a reasonable theoretical explanation has been given for the formation of the observed line structure where $\tau > 0{\cdot}03$. The flow can be interpreted primarily as a balance between pressure and viscous forces, with surface tension exerting, through the boundary conditions, a stabilizing influence. In principle, exactly the same analysis can be carried out for arbitrary functions $h_1(x)$ and $h_2(x)$ and for arbitrary values of M. However, even in the case of circular rollers, the complete solution of equation (18) does not seem readily expressible in terms of tabulated functions, and a complete numerical solution would be laborious. It is, nevertheless, reasonable to suppose that the results of Pitts and Greiller, where $T/\mu U_0 = O(1)$, could be explained using such an analysis. The results of Shaw are to be interpreted as corresponding to the region $\tau \to 0$. It is clear that for this range of values of $T/\mu U_0$, the analysis is unable to represent the secondary flow that occurs; the predicted values of $n(s_{\max})$ tend to infinity and no longer correspond to observed values. This aspect of the problem was discussed in an earlier investigation (Pearson 1957), where it was concluded that the flow pattern in the columns of fluid (figure 3) exerts a dominant influence on the line spacing.

From the purely practical (industrial) point of view, the relevant question to be answered is whether conditions can be so chosen that a stable two-dimensional flow is obtained even for small $T/\mu U_0$. (The trivial answer that a stable flow can be obtained for sufficiently small U_0 is of little assistance.) In most contexts the problem will be tackled and probably solved (or, if not, circumvented) by methods of trial and error, since the possible range of variation of physical circumstances will be strictly limited in any one case.

One method that proves efficient was mentioned in an earlier investigation (Pearson 1957). The roller or wedge is replaced by a flat plate ending in a knife edge. This plate is inclined at a small angle to the horizontal such that $h'(x)$ is negative everywhere, and such that fluid emerges at the point of minimum gap width. Clearly the analysis given above cannot be applied to this case since b_0 will coincide with the end of the plate and $h'(x)$ will be discontinuous at b_0. On the other hand, a simple physical argument in terms of pressure can be given to explain why the flow should be unstable in some cases and stable in others:

consider the flow shown in figure 7 and let b_0 represent the position of the free boundary in a steady two-dimensional flow; if the pressure gradient dp/dx within the fluid is negative near the point $x = b_0$ in the steady two-dimensional case then the result of part of the free boundary moving up to the plane

$$x = b_0 + \delta b \quad (\delta b > 0)$$

is that the induced pressure distribution forces fluid laterally towards these points. In other words, it tends to provide just the excess of fluid that is required to maintain the disturbed boundary. Now, in the case of the roller or the wedge, dp/dx is negative and instability is observed. But where $h'(b_0)$ is negative, as we propose using a knife edge, dp/dx is positive and the flow is inherently stable.

Another technique that has been employed is to make $M = -1$. This again puts the physical circumstances outside the scope of the analysis in §2 because there is now no clear distinction between an upstream and a downstream side. Nevertheless, by putting $t_1 = t_2$ one can obtain a steady solution in which $E(x) \equiv 0$ and by following through the perturbation analysis, it can be shown that the flow is stable provided that $d^2/dx^2(1/h)$ is negative at $x = b_0$. No comparison with observation has yet been made in this case.

An incidental result of this work was that it suggested a new explanation for brush marks. In the past, it had commonly been supposed that these irregularities were due to the nature of the brush itself, formed as it is from a large number of bristles of roughly equal length, the whole assembly being relatively pliable. It now seems as if this is not so and that brush marks are merely a further manifestation of a phenomenon common to most spreading devices.

Since much of the preliminary work on this problem was carried out in the Research Department of Imperial Chemical Industries Limited, Paints Division it is fitting that I should first acknowledge the stimulus given and information provided by Mr C. I. Snow, Mr N. D. P. Smith and Mr A. J. G. Shaw of Paints Division.

Next I wish to express my indebtedness to Sir Geoffrey Taylor who has been kind enough to discuss the problem on numerous occasions and to make available many pieces of information that he has obtained on this and related matters in recent years.

Finally, I wish to thank those members of these laboratories who have helped me with the experimental arrangements—in particular, Miss E. M. Gibbens, who assisted with measurements and calculations, Mr K. D. Cooper who was responsible for most of the photographic arrangements, and the workshop staff who made the spreaders and rollers used here.

REFERENCES

Chalmers, B. & Hoare, W. E. 1941 *J. Iron & St. Inst.*, no. 11.

Hopkins, M. R. 1957 *Brit. J. Appl. Phys.* **8**, 442.

Lamb, Sir H. 1932 *Hydrodynamics*, 6th ed. Cambridge University Press.

Pearson, J. R. A. 1957 Ph.D. Thesis, University of Cambridge.

Pitts, E. 1959 (In the Press.)

Saffman, P. G. & Taylor, Sir Geoffrey 1958 *Proc. Roy. Soc.* A, **245**, 312.

Sjodahl, L. H. 1951 *Amer. Ink Mkr*, **29**, 31.